Communications in Nonlinear Science and Numerical Simulation 117 (2023) 106921

Contents lists available at ScienceDirect

Communications in Nonlinear Science and Numerical Simulation

journal homepage: www.elsevier.com/locate/cnsns

Review

Characterization of chimeras in coupled phase oscillators based on a coherence function

C.A.S. Batista [a,*], S.T. da Silva [b], R.L. Viana [b,c]

[a] Universidade Federal do Paraná, Centro de Estudos do Mar, Pontal do Paraná, Paraná, Brazil
[b] Universidade Federal do Paraná, Departamento de Física, Curitiba, Paraná, Brazil
[c] Universidade de São Paulo, Instituto de Física, São Paulo, SP, Brazil

ARTICLE INFO

Article history:
Received 22 February 2022
Received in revised form 22 August 2022
Accepted 29 September 2022
Available online 10 October 2022

ABSTRACT

In this work we proposed the characterization of chimeras using a mathematical function based on coherent and incoherent states of a chain of spatially distributed oscillators. In particular, the function analyzes the spatial distance between the nearest neighbors in a chain of coupled oscillators. If one site *i* is further away from another site *j*, the function is set to result in an incoherent state and if two sites are close together, a coherent state. The spatial separation is based on a certain threshold. Furthermore, we include the study of spatial correlation in order to observe if there was any correspondence between correlation decay and chimera state formation. To obtain results similar to the coherence function, we also compare the complex order parameter with the coherence function. To develop these studies, we use a Kuramoto-like model in a long-range coupling network.

Contents

1. Introduction 1
2. Kuramoto model with long-range coupling 2
3. Chimera states characterized by spatial correlation 5
4. Characterization of chimeras based in coherent and incoherent function 5
5. Conclusions 8
Declaration of competing interest 9
Data availability 9
Acknowledgments 9
References 10

1. Introduction

Chimera states are a dynamic behavior characterized by the formation of patterns when oscillator groups exhibit incoherent oscillation domains coexisting with coherent dynamics domains. The first studies that characterized this behavior were performed in a coupled chain of nonlinear oscillators [1] Kuramoto and Battogtokh [2] reported the coexistence of coherence and incoherence in nonlocally coupled phase oscillators. Abrams and Strogatz [3] also studied arrays of identical oscillators. Wolfrum and Omel'chenko [4] showed that chimera states can be considered as chaotic

* Corresponding author.
E-mail address: batiscarlos@gmail.com (C.A.S. Batista).

https://doi.org/10.1016/j.cnsns.2022.106921
1007-5704/

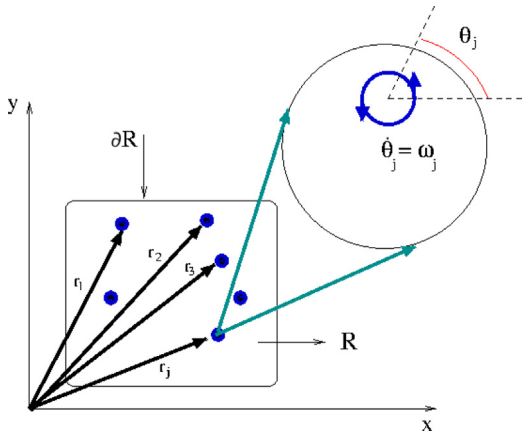

Fig. 1. A system of coupled pointlike oscillators.

transients. In [5] the authors show that amplitude-mediated phase chimeras and amplitude chimeras can occur in the same network of nonlocally coupled identical oscillators

These dynamic features have been found in many dynamical systems [6,7], as well as in coupled mechanical [8,9], chemical [10,11] oscillators and neuronal [12,13] and ecological [14] networks. An experimental evidence was studied by Gambuzza et al. [15] in coupled electronic circuits and by Kapitaniak et al. [16] in coupled pendula. An analytical treatment of transitions from chimeras, where the authors analytically derive the necessary conditions for this transition by means of the coherent stability function approach, is given in Ref. [17].

The non-local coupling used in this work, which is the fast relaxation limit of a more general model of coupling mediated by the diffusion of a chemical substance, is a one-dimensional lattice and is constituted in such a way that its coupling term depends exponentially on a parameter, which can take any real value from zero to infinity and is related to the inverse of the coupling length [18], using the Kuramoto model [19]. Coupled map networks have been considered to model spatially extended dynamical systems [20] and there are various articles in the literature that show chimera states in non-local feature couplings. For example, Omelchenko et all [21], consider a lattice in which exist a specification of the number of neighbors in each direction coupled with the i-th element in the network. In a previous work [22], we characterized chimera in a network of logistic maps connected by means of a smoothed finite range coupling, where it was considered a smoothing of non-local coupling.

The goal of the present paper is to propose a coherence function that identifies numerically when the oscillators are in coherent and incoherent domains. We defined functions that provided us with a snapshot where it is possible to obtain characteristic features which make it possible to distinguish the boundaries of the region in which the existence of chimeras is possible. This function can distinguish in a regime where there is the coexistence of coherent and incoherent states in an instant of time, based on the spatial separation between the i and j phase oscillators. We also considered in our studies the spatial correlation. Such a study inspired us to make an attempt to see if spatial correlation features could provide us with any information about coherent, incoherent, and chimera states.

This paper is organized as follows: In Section 2 we made a description of the coupling form, in which the range of interaction between oscillators decays exponentially and using the Kuramoto model as local dynamics. In Section 3 we developed the first simulations in order to characterize chimeras using the study of spatial correlation. In Section 4 we proposed a characterization of chimeras based in coherent and incoherent states. Finally, in the last section, we express our Conclusions.

2. Kuramoto model with long-range coupling

The mathematical model we deal with in the present work consists of N pointlike phase oscillators, embedded in a d-dimensional Euclidean space, with positions $\mathbf{r}_j$, where $j = 1, 2, \ldots, N$, represented schematically by Fig. 1. Each oscillator is described by a geometrical phase θ_j whose evolution is given by $\dot{\theta}_j = \omega_j$, where ω_j is a frequency randomly chosen from a given probability distribution function $g(\omega)$.

We suppose that the phase oscillators both produce and absorb a given chemical, in such a way that the frequency changes accordingly. Hence, the coupling among oscillators depends on the local concentration of this substance, which is a scalar field denoted by $A(\mathbf{r}, t)$. A general nonlinear coupling is thus represented by the system of differential equations

$$\frac{d\theta_j}{dt} = \omega_j + g(A(\mathbf{r}_j, t)) \qquad (j = 1, 2, \ldots, N), \tag{1}$$

where g is a coupling function.

The chemical mediating the coupling among phase oscillators [23] is supposed to undergo spatial diffusion according to the following equation

$$\frac{\partial A}{\partial t} + \eta\, A - D\,\nabla^2 A = \sum_{k=1}^{N} h(\theta_k)\,\delta(\mathbf{r} - \mathbf{r}_k), \tag{2}$$

where D is the diffusion coefficient, η is a degradation coefficient and there is a source function representing the effect of pointwise oscillators, each of them with a strength given by a function $h()$ of their phases.

The function $h(\theta)$ indicate that the strength of the source depend on the dynamics. For example, depending on the rate of change of θ, the oscillator may oscillate a mediating substance with a different intensity. In order to solve this equation, we specify appropriate boundary conditions at some surface $\partial\mathcal{R}$, as well as an initial condition profile $A(\mathbf{r}, t = 0)$.

The Green function for Eq. (2) is denoted $G(\mathbf{r}, t; \mathbf{r}', t')$ and satisfies

$$\frac{\partial G}{\partial t} + \eta\, G - D\,\nabla^2 G = \delta(\mathbf{r} - \mathbf{r}')\,\delta(t - t'), \tag{3}$$

for homogeneous Dirichlet boundary conditions: $G(\mathbf{r}, t; \mathbf{r}', t')$ for $\mathbf{r} \in \partial\mathcal{R}$, and initial condition $G(\mathbf{r}, t = 0; \mathbf{r}', t') = 0$. The solution of the inhomogeneous diffusion equation (2), for absorbing boundary conditions in $\partial\mathcal{R}$ and initial profile $A(\mathbf{r}, t = 0) = 0$, is given by

$$A(\mathbf{r}, t) = \sum_{k=1}^{N} \int_0^{t^+} dt'\, h(\theta_k(t'))\, G(\mathbf{r}, t; \mathbf{r}_k, t'). \tag{4}$$

We remark that $A(\mathbf{r}, t)$ is the local concentration of the substance causing the coupling, the function g expresses the influence of the local concentration on the oscillator dynamics. For example, if the concentration is higher, then the oscillator experiences greater external forcing due to coupling with other oscillators, which in turn are producing the mediating substance. The coupling results from the exchange existing between the oscillators that at the same time produce and absorb the substance.

Substituting this solution into Eq. (1) and choosing, for simplicity, a linear and time-independent coupling function $g()$, there results a system of integro-differential equations governing the coupling among phase oscillators mediated by the diffusion of a substance

$$\frac{d\theta_j}{dt} = \omega_j + \sum_{k=1}^{N} \int_0^{t} dt'\, H(\theta_k(t'))\, G(\mathbf{r}_j, t; \mathbf{r}_k, t') \qquad (j = 1, 2, \ldots, N), \tag{5}$$

where we defined the composite function $H() = g(h())$. A generalized Kuramoto model is obtained by choosing

$$H(\theta_j) = (K/N)\sin(\theta_k - \theta_j), \tag{6}$$

where $K > 0$ is a coupling strength, for which (5) reads

$$\frac{d\theta_j}{dt} = \omega_j + \frac{K}{N} \sum_{k=1}^{N} \int_0^{t} dt'\, \sin[\theta_k(t') - \theta_j(t')]\, G(\mathbf{r}_j, t; \mathbf{r}_k, t') \qquad (j = 1, 2, \ldots, N), \tag{7}$$

The Dirichlet Green function for a one-dimensional oscillator chain with free boundary conditions is

$$G(x, t; x', t') = \frac{\Theta(t - t')}{\sqrt{4\pi(t - t')}} \exp\left[-\eta\,(t - t') - \frac{(x - x')^2}{4D(t - t')}\right] \tag{8}$$

where $\Theta(t - t')$ is the Heaviside unit-step function. Other cases, in two and three dimensions, and with finite domains with absorbing boundaries, can be found in [24]. Inserting this expression into (7) yields

$$\frac{d\theta_j}{dt} = \omega_j + \frac{K}{N} \sum_{k=1}^{N} \int_0^{t} dt'\, \frac{\sin[\theta_k(t') - \theta_j(t')]}{\sqrt{4\pi(t - t')}} \exp\left[-\eta\,(t - t') - \frac{(x_j - x_k)^2}{4D(t - t')}\right]. \tag{9}$$

Let us consider a regular chain of phase oscillators, occupying fixed positions in a one-dimensional lattice with the same distance Δ between adjacent sites, such that $x_j = j\Delta$, with $j = 1, 2, \ldots, N$ and $\Delta = 1$. In this chain we impose periodic boundary conditions, i.e. $\theta_j = \theta_{j\pm N}$ for any j. We choose an initial condition profile for this lattice, $\theta_j(t = 0)$, e.g. randomly chosen phases in the interval $[0, 2\pi)$. We also suppose that the oscillator frequencies ω_j are randomly selected from a Gaussian probability distribution with zero mean and unit variance. A full solution of the system (9) requires that, at each time t, we include the contribution of all oscillators in all times $t' < t$ in order to compute the time integral which contains the Green function. After this, we evolve the system of coupled differential equations by a single integration step, and repeat all this computation. This is clearly a very time-consuming task, and numerical results have been obtained so far for a small number N of oscillators.

If we consider the limit of very fast diffusion, however, the equations simplify considerably because the phase oscillators are instantaneously affected by the concentration of the coupling-mediating chemical. In other words, this concentration attains its equilibrium value so rapidly that no time-integration would be required in the coupling term. Formally, this is equivalent to take the $t \to \infty$ limit in the interaction kernel

$$\sigma(x_j, x_k; t) = \int_0^t dt' \, G(x_j, t; x_k, t'). \tag{10}$$

Using the Green's function given by (8) we obtain

$$\sigma(x_j, x_k; t) = \int_0^t dt' \, \frac{e^{-\eta(t-t')}}{\sqrt{4\pi D(t-t')}} \exp\left[-\frac{(x_j - x_k)^2}{4D(t-t')}\right]. \tag{11}$$

Performing a change of variables, we have

$$\sigma(x_j, x_k; t) = \frac{x_j - x_k}{4D\sqrt{\pi}} \int_{u_1}^{\infty} \frac{du}{u^{3/2}} \exp\left(-u - \frac{a_1}{u}\right), \tag{12}$$

where

$$a_1 = \frac{\eta(x_j - x_k)^2}{4D} = \left\{\frac{\gamma(x_j - x_k)}{2}\right\}^2, \qquad u_1 = \frac{(x_j - x_k)^2}{4Dt}, \tag{13}$$

and we have defined a coupling length

$$\gamma = \sqrt{\frac{\eta}{D}}. \tag{14}$$

The fast diffusion case is equivalent to take the $t \to \infty$ limit for the interaction kernel, for which $u_1 \to 0$:

$$\sigma(x_j, x_k) = \lim_{t\to\infty} \sigma(x_j, x_k; t) = \frac{\gamma}{2\eta} \exp\left\{-\gamma(x_j - x_k)\right\}, \tag{15}$$

which coincides with the earlier results of Kuramoto and coworkers [25,26]. Therefore, in the fast diffusion limit, the equations governing the time evolution of a coupled one-dimensional chain of phase oscillators are

$$\frac{d\theta_j}{dt} = \omega_j + KC(\gamma) \sum_{k=1}^{N} e^{-\gamma\Delta(j-k)} \sin(\theta_k - \theta_j) \qquad (j = 1, 2, \ldots, N), \tag{16}$$

where $C(\gamma)$ is an overall normalization constant introduced for consistency of the coupling term and periodic boundary conditions $\theta_j = \theta_{j+N}$. We can rewrite the summation to consider symmetric pairs of neighbors separated by a lattice distance $\ell\Delta$, where $\ell = \min|j-k|$. ω_i is the natural frequency of the *ith* oscillator chosen at random from a Gaussian probability density.

In this work, we used the Kuramoto model in a network with long-range coupling, which is composed by an exponential term that mimetizes a diffusing chemical substance

$$\frac{d\theta_j}{dt} = \omega_j + KC \sum_{l=1}^{N'} e^{-\gamma\Delta l}[\sin(\theta_j - \theta_{j-l}) + \sin(\theta_j - \theta_{j+l})], \tag{17}$$

where the constant Δ is a distance between consecutive lattice sites, $l = 1, 2, \ldots, N'$, C is normalization constant

$$C = \left[2\sum_{l=1}^{N'} e^{(-\gamma\Delta l)}\right]^{-1} \tag{18}$$

and $N' = \frac{N-1}{2}$.

In particular, if γ goes to zero then

$$C = \frac{1}{2N'} = \frac{1}{N-1}, \tag{19}$$

and we have an all to all (or global) type of coupling. In other hand, if γ is large,

$$C \approx \frac{1}{2e^{-\gamma\Delta}}, \tag{20}$$

and (17) becomes a nearest neighbors (or local) coupling.

The equations of the coupled model were integrated numerically using a fourth order fixed step size Runge–Kutta method, periodic boundary conditions and sinusoidal initial conditions.

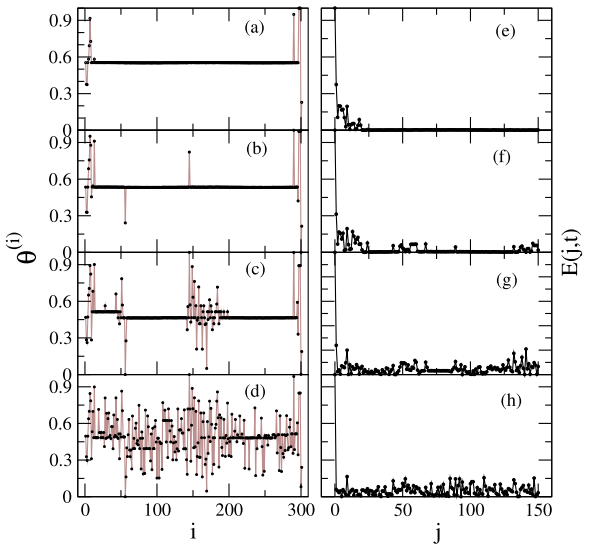

Fig. 2. Snapshots of the spatial pattern for the coupled lattice for $\gamma = 0.002$, $t = 2000$ and $N = 301$ in (a), (b), (c) and (d), where $K = 12$, $K = 9$, $K = 7$, $K = 5$, respectively. Spatial Correlation for (e), (f), (g) and (h), where $K = 12$, $K = 9$, $K = 7$, $K = 5$, respectively.

3. Chimera states characterized by spatial correlation

As described in the Introduction, chimera states are characterized by the combination of coherent and incoherent oscillations. So our first step is to use a spatial correlation function [27]

$$E(j,t) = \frac{(1/N)\sum_{i=1}^{N} \hat{\theta}_t^{(i)} \hat{\theta}_t^{(i+j)}}{(1/N)\sum_{i=1}^{N} (\hat{\theta}_t^{(i)})^2}, \tag{21}$$

where $\langle\theta\rangle = (1/N)\sum_{i=1}^{N} \theta_t^{(i)}$ is the spatial average for the lattice, and $\hat{\theta}_t^{(i)} = \theta_t^{(i)} - \langle\theta\rangle_t$ are the deviations from this average. The correlation function decays with the value of distance j in the network. This definition follows the properties of the temporal correlation function. The Fig. 2 shows the results of the simulations where in the left column we plotted some profiles that showed different behaviors, in which we varied the coupling strength K. They change from coherent states [Fig. 2(a)], chimeras states [Fig. 2(b) and (c)] to completely incoherent states [Fig. 2(d)]. What we see in the column on the right, where we plot correlation, is it provided considered information. Analyzing at the spatial correlation, in the column on the right, it showed a strong decay for all cases. The spatially incoherence regions in the lattice are characterizing by a fluctuating behavior of $E(j,t)$.

In Fig. 3 we repeat show the similar results about the spatial correlation, but the coupling parameter is fixed value and choiced different values for γ parameter. We observe a behavior analogous to Fig. 2. Starting from a determined value ($\gamma = 0.002$), the behavior of the oscillators presented a coherent state of oscillation as shown in Fig. 3(a). Increasing the γ-value the chimera states appear as shown in Fig. 3(b) and (c), until the state of total incoherent oscillations Fig. 3(d). In the right column of Fig. 3, from (e) to (h), where we plotted the corresponding spatial correlations. Our simulations about the decay of $E(j,t)$ are the same as for Fig. 2(e) to (h).

In our analysis the number of incoherent states increase, as shown in the left panels of Figs. 2 and 3 (from top to bottom), there is a correspondence in the small fluctuations of the spatial correlation function. Using $E(j,t)$ we could relate a characterization of coherent and incoherent states, but this characterization is incomplete when there are chimeras. When calculating the spatial correlation, it is only possible to be sure when the oscillators are completely coherent or completely incoherent. The coexistence of these states, which characterizes a chimera, cannot be adequately quantified using a spatial correlation function. We propose this characterization in the next section, a different quantifier through a coherence function.

4. Characterization of chimeras based in coherent and incoherent function

In this section, we introduce a function to characterize chimeras in a determined condition using a mathematical tool based on a Heaviside function. A similar technique was used to recurrence plots, studied in [28]. Let $\theta_t^{(i)}$ and $\theta_t^{(j)}$ be the values of the oscillators phases at sites i and j at a fixed time t. We first compute the quantity

$$\phi_{i,j}(\varepsilon, t) = H(\varepsilon - \|\theta_t^{(i)} - \theta_t^{(j)}\|), \tag{22}$$

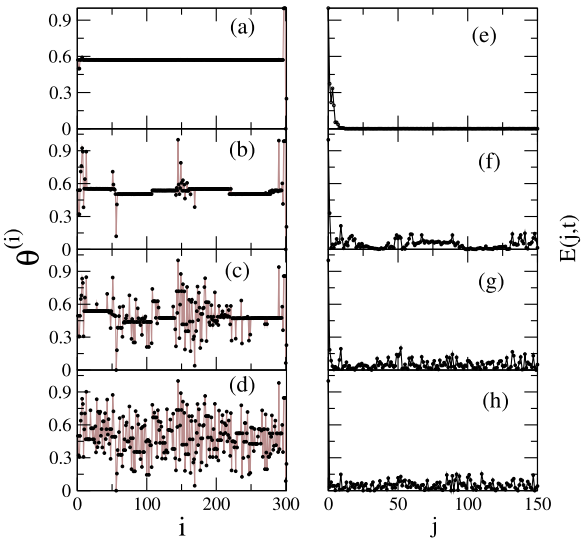

Fig. 3. Snapshots of the spatial pattern for $N = 301$, $K = 12$ and $n = 2000$ in (a), (b), (c) and (d), where $\gamma = 0.002$, $\gamma = 0.004$, $\gamma = 0.006$, $\gamma = 0.01$, respectively. Spatial Correlation for (e), (f), (g) and (h), where, $\gamma = 0.002$, $\gamma = 0.004$, $\gamma = 0.006$, $\gamma = 0.01$, respectively.

where H is the Heaviside function and when the spatial difference between a site i and another site j is greater than a determined threshold distance ε, we have an incoherent state. If this difference is smaller than ε characterize a coherent state in a snapshot. In this way, we defined a coherence function $\phi(\varepsilon)$ from of Eq. (22):

$$\Phi(\varepsilon) = \sum_{i,j=1}^{N'} \frac{N - \phi_{i,j}(\varepsilon, t)}{N}, \tag{23}$$

where N is the size of network and $N' = (N-1)/2$. Where we set up a given $\varepsilon = 0.02$, the sum can take values between 0 and 1. It will be either zero if all states are incoherent, a real number between 0 and 1 given by the ratio between coherent and incoherent states, and unity if all states are coherent. In Fig. 4 we presented results of numerical simulations for the function $\Phi(\varepsilon)$ varying the main parameters of the system. In Fig. 4(a) we plotted the spatial coherence function in terms of coupling strength K parameter. We observed that there is a dependence of $\Phi(\varepsilon)$ with coupling strength revealing a transition from a completely incoherent to a fully coherent state, for large K. K increases, the degree of coherence given by Φ varies from values close to zero, for completely incoherent states and approaches the unit, that characterize nearly complete coherent states. There is a particular result in this figure, for $\gamma = 0.01$, that depending on some parameters of the system, even increasing the coupling force it is not possible to reach coherent states at least for the range of K we considered here. In Fig. 4(b) we set some values of K, and vary the parameter γ. We find a dependence that agrees with the limiting cases of our non-local model. They are: (i) the global coupling case, for $\gamma = 0$ [Eq. (19)] and (ii) the nearest-neighbor coupling (large γ) case [Eq. (20)]. As we increase the parameter γ the structure of the network changes from a global coupling to a local coupling. In global couplings, all oscillators interact with each other. So coherent states are easier to obtain in global coupling. However, local couplings in coherent states are very difficult to obtain in lattices where the local coupling is characterized.

In the same way, we defined a chimera function Φ_c

$$\Phi_c(\varepsilon) = \sum_{i,j=1}^{N'} \frac{N - \phi_{i,j}(\varepsilon)}{N}, \tag{24}$$

which is analogous to the previous definitions, but we limit its calculation to the pairs of oscillators for which range $L_i < \Phi_{i,j}(\varepsilon) < L_s$ given the lower and upper limits L_i and L_s. It will just be calculated when the inferior limit is $L_i = E_s$ where E_s is a determined number of coherent states and the superior limited L_S is $L_s = N - E_s$. In our simulations, we used $E_s = 15$. This assertion was defined due to the function Φ reaching from totally coherent and totally incoherent states. It provides the spatial coherence of the entire network at snapshot. Fully coherent states are not characterized by chimeras, there are necessarily coherent and incoherent states in a snapshot. The same goes for totally incoherent states. But with the definition of Φ_c we can get chimera states for some values of the system parameters, as shown in Fig. 5. In the blue shaded area given for Φ_c, we have all values for which the system presents chimeras states. In Fig. 5(a) we can see that chimeras states happens only if $\approx (5 \leq K \leq 17.2)$, when varying the K parameter. What differs from the black line, given by Φ, which represents the degree of coherence. In Fig. 5(b) we plotted the dependence of functions in

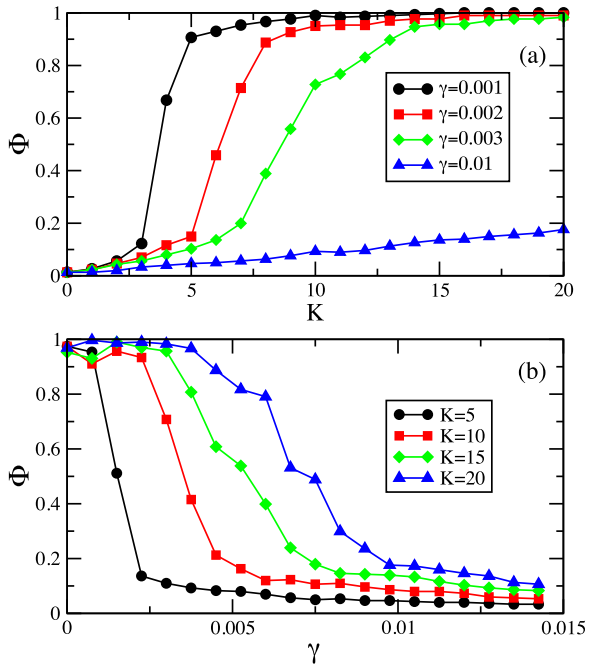

Fig. 4. Coherence function Φ for $N = 301$ and $t = 2000$: (a) *versus* strength force K. (b) *versus* exponential parameter γ.

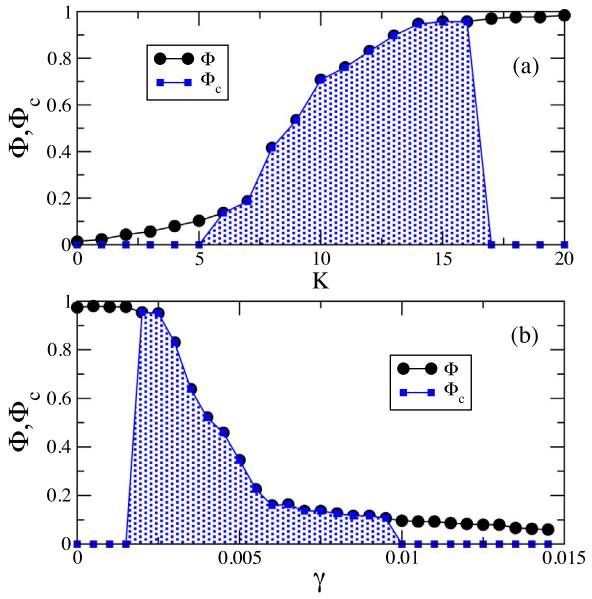

Fig. 5. Coherence Function Φ and Chimera Function Φ_c, for $K = 12$ and $t = 2000$: (a) *versus* strength force K and $\gamma = 0.003$. (b) *versus* exponential parameter γ.

terms of γ parameter, and it presents the same behavior, where a region determined of chimeras states, given for Φ_c is less than all the region of Φ studied.

In order, we studied the regions in Fig. 5 for to validate the proposition of chimera function. The results are present in Fig. 6. In the left column, for (a) to (d), the snapshots are related with the figure Fig. 5(a). So, for $K = 2$ and $K = 18$ there are only incoherent and coherent states, respectively. However, for $K = 8$ and $K = 11$ the snapshots exhibit the chimera states, according to our definition of Φ_c. The same was verified for the results of the column to the right. For $\gamma = 0.001$ and $\gamma = 0.01$ there are only coherent states and full incoherent states, respectively. For $\gamma = 0.003$ and $\gamma = 0.05$, chimeras states.

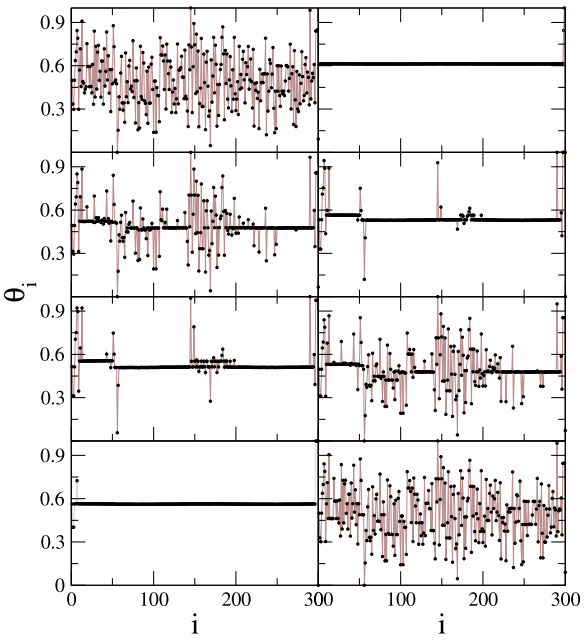

Fig. 6. Snapshots of the spatial pattern for $N = 301$ and $t = 2000$. In (a) $K = 2$, (b) $K = 8$, (c) $K = 11$ and (d) $K = 18$. For (e) $\gamma = 0.001$, (f) $\gamma = 0.003$, (g) $\gamma = 0.005$ and (h) $\gamma = 0.01$.

In order to compare the behavior of the coherence function with quantifiers, we also compute the Kuramoto complex phase order parameter [29]. Let $\Theta^{j}_{(t)}$ be the phase of the jth oscillator for a time t. Then we define

$$z(t) = R(t)\exp(i\Theta(t)) \equiv \frac{1}{N}\sum_{j=1}^{N}\exp(i\theta_t^{(j)}), \tag{25}$$

where R and Θ are the amplitude and angle, respectively, of a centroid phase vector for a one-dimensional lattice with periodic boundary conditions. In certain cases, it is possible to obtain analytically same aspects of the behavior in the $N \to \infty$ limit, by using the Ott–Antonsen approach, is more details can be found in [30,31]. A comparison with our results showed that there is a similar behavior from a qualitative point of view with respect to the existence of coherent and incoherent states. For completely synchronized states, what constitutes a totally coherent state, the value of R is nearly to the unity ($R \approx 1$). On the other limit, if the state are completely non synchronized $R \approx 0$, that this can be considered a full incoherent state chimeras are thus profiled for $0 < R < 1$. However, for a more rigorous analysis, in Fig. 7(a) the order parameter decays faster compared to the coherence function and with some fluctuations. In Fig. 7(b) the transition of the coherence function is more abrupt than the order parameter. In both cases, the coherence function can identify in more detail certain dynamics in a network of oscillators. However, we must remember that the order parameter is related to the phase and the coherence function to the spatial distance of the oscillators.

Finally, we perform a study in parameters space of the coherence function Φ. In Fig. 8(a) the color bar represents the coherence function Φ and Fig. 8(b) the color palette represents the chimera function Φ_c. When the parameter γ takes on high values, the coherence function is very low, showing that there are practically only incoherent states. As far as synchronization in concerned, networks that characterize local coupling are not good for synchronization [32–34]. But when γ is low, (global coupling characterize), the values of the coherence function are higher, because globally coupled lattices are relative easier to synchronize. The regions that present chimeras states are well-defined.

5. Conclusions

The study objective of the study presented in this article was to propose an alternative tool to identify chimera states in a network of coupled oscillators, using the spatial separation between nearest neighbor oscillators. We use the model to study chimeras in which the coupling is mediated by a diffusive substance with application in biological systems. For example, where the interaction between dynamically active cells is mediated by a chemical that diffuses through the intercellular medium. In our model, however, the diffusive is characterized by a range of parameters γ In this context, the γ parameter provides a way where we can describe from global (all-to-all) to local (closest neighbors) characteristics of the network coupling, as limiting forms of non-local coupling.

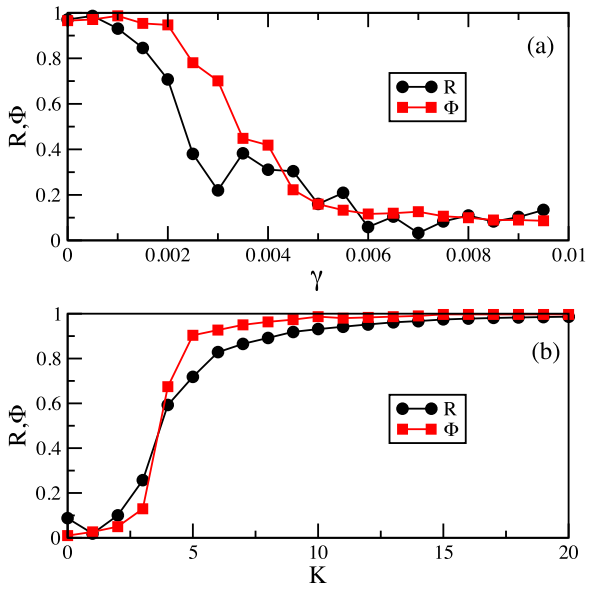

Fig. 7. Comparative of order parameter (black circles) and coherence function (red squares) for $N = 301$ and $t = 2000$. In (a) $K = 10$ and (b) $\gamma = 0.001$.

The transition from incoherent to coherent states depends on non-local coupling characteristics for a fixed coupling force. That is, if the factor γ is very small (tending to zero) the oscillators showed coherent dynamics. On the other hand, as γ is increased, incoherent states grew in a given proportion. In the case for a certain fixed value of the γ-parameter, the increase of the coupling force between the oscillators makes the dynamics of the oscillators to evolve from incoherent to coherent states.

For a fixed value of γ the variation of the coupling strength resulted in a transition from incoherent states to coherent states. Since both the γ factor and the coupling influence the coherence of the oscillators pattern, allowed us to identify the respective states by our definitions of the coherence functions. Firstly, the coherence function, which gave us all the oscillator states, and secondly, the chimera function Φ_c, for which the restriction of the coherence function identify the existence of chimera states. Such features have not possible to observe in the studies of the spatial correlation function.

The inclusion of the spatial correlation function and the Kuramoto order parameter, well-known quantifiers in the literature, helped us to develop our analyses. In particular, the comparison of our results with those with the order parameter, showed that there was a similarity in the behaviors, but the coherence function managed to identify some distinct regions of coherent and incoherent states beyond what the order parameter presented.

Furthermore, the coherence function allowed us to use the system parameters in a wide region where we could characterize whether the oscillators were in fully coherent/incoherent states and a combination of them where it was defined as chimera states. Finally, the present study can also be used for other models, of problems of physical and biological interest. For example, in the interaction mediated by a chemical the brain cells responsible by the circadian rhythm, which is a collective behavior that be compared in this work.

Declaration of competing interest

The authors declare that they have no known competing financial interests or personal relationships that could have appeared to influence the work reported in this paper.

Data availability

The data that has been used is confidential.

Acknowledgments

This work has been partially supported by the Brazilian Government Agencies CNPq. (Grants N^o 403120/2021 − 7 and 301019/2019 − 3), FAPESP, Brazil (Grant 2022/04251 − 7) and CAPES, Brazil (Grant 88881.143103/2017 − 01)

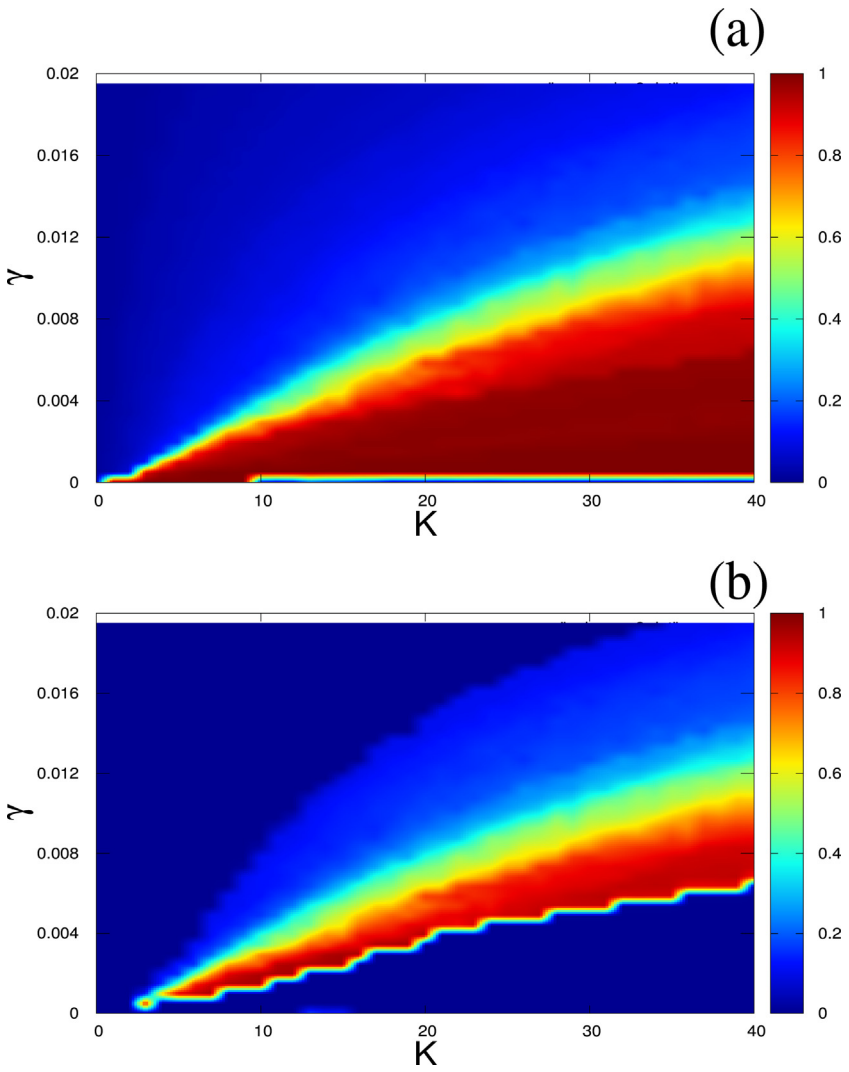

Fig. 8. Parameters space $\gamma \times K$ for $N = 301$ and $t = 2000$. (a) Coherence function Φ and (b) Chimeras function Φ_c.

References

[1] Umberger DK, Grebogi C, Ott E, Afeyan B. Phys Rev A 1989;39:4835. http://dx.doi.org/10.1103/PhysRevA.39.4835.
[2] Kuramoto Y, Battogtokh D. Nonlinear Phenom Complex Syst 2002;5:380.
[3] Abrams DM, Strogatz SH. Phys Rev Lett 2004;93:174102. http://dx.doi.org/10.1103/PhysRevLett.93.174102.
[4] Wolfrum M, Omel'chenko OE. Phys Rev 2011;84:015201. http://dx.doi.org/10.1103/PhysRevE.84.015201.
[5] Banerjee T, Biswas D, Ghosh D, Schöll E, Zakharova A. Chaos 2018;28:113124. http://dx.doi.org/10.1063/1.5054181.
[6] Santos MS, Szezech Jr JD, Batista AM, Caldas IL, Viana RL, Lopes RS. Phys Lett A 2015;379:2188. http://dx.doi.org/10.1016/j.physleta.2015.07.029.
[7] Santos V, Szezech Jr JD, Batista AM, Iarosz KC, Baptista MS, Ren HP, Grebogi C, Viana RL, Caldas IL, Maistrenko YL, Kurths J. Chaos 2018;28:081105. http://dx.doi.org/10.1063/1.5048595.
[8] Martens EA, Thutupalli S, Fourriére A, Hallatschek O. Proc Natl Acad Sci USA 2013;110:10563. http://dx.doi.org/10.1073/pnas.1302880110.
[9] Kapitaniak T, Kuzma P, Wojewoda J, Czolczynski K, Maistrenko Y. Sci Rep 2014;4:6379. http://dx.doi.org/10.1038/srep06379.
[10] Tinsley MR, Nkomo S, Showalter K. Nat Phys 2012;8:662. http://dx.doi.org/10.1038/nphys2371.
[11] Nkomo S, Tinsley MR, Showalter K. Phys Rev Lett 2013;110:244102. http://dx.doi.org/10.1103/PhysRevLett.110.244102.
[12] Santos MS, Szezech Jr JD, Borges FS, Iarosz KC, Caldas IL, Batista AM, Viana RL, Kurths J. Chaos Solitons Fractals 2017;101:86. http://dx.doi.org/10.1016/j.chaos.2017.05.028.
[13] Santos MS, Protachevicz PR, Iarosz KC, Caldas IL, Viana RL, Borges FS, Ren HP, Szezech Jr JD, Batista AM, Grebogi C. Chaos 2019;29:043106. http://dx.doi.org/10.1063/1.5087129.
[14] Banerjee T, Dutta PS, Zakharova A, Schöll E. Phys Rev E 2016;94:032206. http://dx.doi.org/10.1103/PhysRevE.94.032206.
[15] Gambuzza LV, Buscarino A, Chessari S, Fortuna L, Meucci R, Frasca M. Phys Rev E 2014;90:032905. http://dx.doi.org/10.1103/PhysRevE.90.032905.
[16] Kapitaniak T, Kuzma P, Wojewoda J, Czolczynski K, Maistrenko Y. Sci Rep 2016;6:34329. http://dx.doi.org/10.1038/srep06379.
[17] Rakshit S, Faghani Z, Parastesh F, Panahi S, Jafari S, Ghosh D, Perc M. Phys Rev E 100 012315 http://dx.doi.org/10.1103/PhysRevE.100.012315.
[18] Batista CAS, Szezech b Jr JD, Batista AM, Macau EEN, Viana RL. Physica A 2017;470:236–48. http://dx.doi.org/10.1016/j.physa.2016.11.140.

[19] Kuramoto Y. Chemical oscillations, waves, and turbulence. Berlin-Heidelberg-New York-Tok.
[20] Kaneko K. Physica D 1989;34:1. http://dx.doi.org/10.1016/0167-2789(89)90227-3.
[21] Omelchenko I, Maistrenko Y, Hövel P, Schöll E. Phys Rev Lett 2011;106:234102. http://dx.doi.org/10.1103/PhysRevE.85.026212.
[22] Batista CAS, Viana RL. Chaos Solitons Fractals 2020;131:109501. http://dx.doi.org/10.1016/j.chaos.2019.109501.
[23] Kuramoto Y. Progr Theoret Phys 1995;94:321–30. http://dx.doi.org/10.1143/PTP.94.321.
[24] Aristides RP, Viana RL. Nonlinear Dynam 2020;100:3759. http://dx.doi.org/10.1007/s11071-020-05700-9.
[25] Kuramoto Y, Nakao H. Physica D 1997;103:294–313. http://dx.doi.org/10.1016/S0167-2789(96)00264-3.
[26] Kuramoto Y, Nakao H. Phys Rev Lett 1996;76:4352. http://dx.doi.org/10.1103/PhysRevLett.76.4352.
[27] Vasconcelos DB, Viana RL, Lopes SR, Batista AM, Pinto SEde S. Physica A 2004;343:201. http://dx.doi.org/10.1016/j.physa.2004.06.063.
[28] Santos MS, Szezech Jr JD, Batista AM, Caldas IL, Viana RL, Lopes SR. Phys Lett A 2015;379:2188. http://dx.doi.org/10.1016/j.physleta.2015.07.029.
[29] Kuramoto Y. Chemical oscillations, waves and turbulence. New York: Dover; 2003.
[30] Ott Edward, Antonsen Thomas M. Chaos 2008;18:037113. http://dx.doi.org/10.1063/1.2930766.
[31] Barioni AED, de Aguiar MAM. Chaos 2021;31:113141. http://dx.doi.org/10.1063/5.0069350.
[32] Anteneodo C, Batista AM, Viana RL. Physica D 2006;223:270–5. http://dx.doi.org/10.1016/j.physd.2006.10.001.
[33] Anteneodo C, Batista AM, Viana RL. Phys Lett A 2004;326(3–4):227–33. http://dx.doi.org/10.1016/j.physleta.2004.04.035.
[34] Anteneodo C, de S. Pinto SE, Batista AM, Viana RL. Phys Rev E 2003;68. 045202(R); Phys. Rev. E 2004;69. 045202(E) Erratum:.